

A high-voltage power electronics unit for flying insect robots that can modulate wing thrust

Johannes James¹, Sawyer Fuller¹

Abstract—Flapping-wing insect-scale robots (<500 mg) offer enormous potential advantages over larger robots in applications such as agricultural support, environmental monitoring, and exploration of hazardous locations or extra-terrestrial space. Scaling laws that confer advantages to smaller robots, such as reduced materials cost and lower power requirements, also pose miniaturization challenges. Here we address the challenge of supplying a high voltage, oscillating signal to piezoelectric actuators that can be modulated to vary wing thrust. We present a system capable of modulating thrust for the generation of forces and torques required for control of flapping-wing insect sized robots. The power electronics unit with boost converter and two drivers is 90 mg including optional 15 mg output storage capacitor (not including 8 mg MCU). The boost converter operates at 30–40% efficiency at 240 V output under driver load and supplied with 7 V, and the driver produces sinusoidal wing flapping signals at typical operating output voltages of 160–220 V_{pp} with <14% total harmonic distortion. The system can linearly modulate measured thrust over 70% of the tested amplitude range from 40–200 V_{pp} . The thrust modulation reported here is necessary to realize controlled flight using on-board power systems, instead of externally provided signals via a wire tether.

I. INTRODUCTION

A critical aspect of any control system is the actuation. This is especially true for the fast and unstable dynamics of lightweight flying insect-sized robots (FIRs) such as [1] (Fig. 1). It was demonstrated in [2] that bimorph (two-layer) bending beam piezoelectric actuators can be used to flap the wings of FIRs and achieve stable flight control, but these ‘flight muscles’ require precise high voltage electrical signals. To date, flight control demonstrations of piezo-actuated robots have required benchtop piezo amplifiers (e.g. Trek model 2205 in [3]). These serve to amplify the low voltages (e.g. 0–5 V) produced by the flight control system to 200–300 V required by the piezoelectric actuators. Alternatives to piezoelectric actuation that do not have a high voltage requirement, such as electromagnetic coils [4], [5] have not yet demonstrated sufficient power density or independent wing control at the size scale we are concerned with here (less than 500 mg).

This work is concerned with the technology needed to move the high voltage signal generator on-board the robot, that is, creating an on-board power electronics unit (PEU). We assume the bimorph piezoelectric actuators will be driven in ‘simultaneous drive’ mode to provide a balance between low weight and efficiency [6]. In simultaneous drive, the two outer surfaces of the piezo cantilevers are held at a fixed

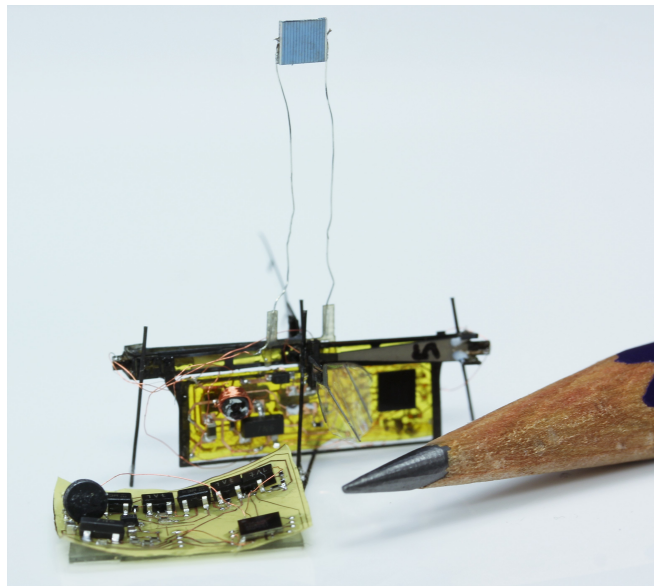


Fig. 1: The UW Robofly shown with flight-weight power electronics, on-board PV cell power source, and microcontroller. A pencil tip is shown for scale. Shown at lower left is a flight-weight implementation of the updated power electronics unit (PEU) reported here that additionally features two complete half-bridge drivers for independent dual-wing control.

potential difference, V_{Bias} , while the middle layer between the two piezos is excited by a unipolar sinusoidal signal V_{Sig} (Fig. 2). Motivated by a plan to eventually bring the PEU on-board, the flight control demonstrations of [7], [2], [1] all used piezo actuators in simultaneous drive configuration.

By careful control of the bias voltage V_{Bias} and the sinusoidal flapping signal V_{Sig} , the resulting time-varying electric field across both layers of the bending-beam bimorph actuators produces actuator tip motion according to the inverse piezoelectric effect. This in turn moves the wings through a high-ratio cantilever arm in the transmission. Modifications to the baseline sinusoid V_{Sig} , such as changes in its amplitude V_{pp} , DC offset, and adding a second harmonic, can produce all of the torques and forces necessary to control a two-winged FIR in flight [8], [2]. Furthermore, it has been recently shown that these same signal perturbations are sufficient to actuate FIRs underwater [9] and on the ground and the surface of the water [1].

Using benchtop piezo amplifiers, connected to the FIR through a thin wire tether, is convenient to demonstrate functionality of the flight actuation apparatus [10], [2]. This

¹Authors are with the Department of Mechanical Engineering, University of Washington, Seattle, WA 98195, USA jm james@uw.edu

is because high voltage, low-impedance amplifiers are commercially available in form factors suitable for the benchtop. However, use of a wire tether is clearly undesirable because of how it limits the useful range of the robots and confounds many aspects of flight control [7].

There are smaller, commercially available piezo drivers, but they are either too heavy for FIRs which weigh < 200 mg or not suitable for driving bimorph actuators at sufficiently high voltage. Boréas Technologies, (Bromont, QC, Canada) offers piezo driver ICs such as BOS1901 which stem from [11] and are impressively efficient and within SWaP constraints of FIRs. But these can generate a maximum $190 V_{pp}$ differential drive signal (*not* ground referenced) and don't supply a bias rail in this higher voltage operation mode. Alternatively, custom power electronics using discrete components provide design flexibility and can meet design needs within size, weight, and power (SWaP) constraints. Such custom flight-weight power electronics have been presented [6] and utilized [12], [13]. Recently, progress has been made in on-board power systems on FIRs such as the UW Robofly [12] and the Harvard Robobee [13]. These robots were *powered* wirelessly. However, their flights were in open loop, that is, with *uncontrolled* flapping, resulting in very short flights, all of which were less than a second.

Here, we report an advance in this area by demonstrating a system that is small enough (≈ 90 mg not including controller) to fly on an FIR that can also modulate its output waveform in a way that can, repeatably, vary the thrust output of the flapping wings. The waveform it produces is close to a pure sinusoid. This avoids exciting high-frequency self-bending modes of the piezoelectric actuators that can induce high strains reduce efficiency. Of particular importance, this can reduce cracking [14].

Because roll torque for the UW Robofly [7], [3], [15], [1] is based on body geometry and wing placement, a linear actuator for thrust force given commanded flapping amplitude is prerequisite for attitude and position control of the robot in flight. This waveform generator can also be used to drive the DC offset and additional harmonic content of V_{sig} needed for both pitch and yaw torques, as discussed in [2], [16], [1].

II. ROBOT HARDWARE

Physical Instantiation

Experiments were performed with, and our system design targets, application on an enlarged version of the UW Robofly that was first introduced in [3]. Key differences from its predecessor [1], [12] are a widened actuator and reoriented actuator to improve control authority and increase lift. Each of its two wings is coupled to an assembly that consists of a piezoelectric cantilever and a rigid airframe and flexure-based transmission made of laser-micromachined carbon fiber composite. In such designs, whose passive wing hinge traces its lineage to [10], careful mechanical design of the actuator, transmission, and wing hinge is needed to ensure that the angle of attack and piezo system maximize both lift and efficiency [17], [18].

It is worth remarking in passing that even though the system is operated at mechanical resonance, its small scale precludes voltage amplification through an AC transformer or configuration in electrical resonance. This is because the relatively low flapping frequency (100–200 Hz) would require prohibitively large inductors.

On-board Power Electronics (PEU)

On the benchtop, high-voltage linear amplifiers are able to drive a wide variety of piezo actuator configurations under unpredictable loading conditions because they have high gain, fast feedback, and low output impedance. This approach has the benefit of convenience but it is impossible for a PEU within the SWaP constraints of an FIR due to the high component count and excessive weight of high-voltage and high-gain linear amplifier circuitry in either discrete or IC form.

Our system instead relies on an on-board microcontroller operating the PEU in pulse frequency modulation (PFM) and using digital feedback. This reduces the component count, but entails overcoming other sources of difficulty:

- 1) obtaining fast and accurate measurements for feedback control of the high-voltage output. Voltage divider trade-offs between equivalent impedance vs. output range and noise. I_{Bias} and I_{sig} are difficult to measure on the FIR due to the need for large amplification, filtering, and difficulty of miniaturized high-side current measurement
- 2) coupling between V_{Bias} and V_{sig} because current for V_{sig} is drawn from V_{Bias} and the capacitive coupling of the piezoelectric actuator layers
- 3) variable authority in the driver stage for both the high-side and low-side, that depend on the instantaneous voltage differentials $V_{Bias} - V_{sig}$, $V_{sig} - gnd$, respectively.
- 4) unpredictable range of power draw depending on dynamic loading, which is a function of highly complex and incompletely understood fluid mechanics of flapping wing insect flight.
- 5) unpredictable power factor, which is a function of dynamic actuator impedance, wing mechanism inertia, and aerodynamic forces
- 6) limited on-board computational resources

We outline in Section III how these were overcome.

Two basic power conversion & driving topologies have demonstrated promising results in piezo-actuated FIRs with discrete as opposed to monolithic ([19], [20]) PEUs:

- 1) Boost converter and half-bridge driver for bimorph actuators in simultaneous drive. It was proposed for FIRs in [21] and used for the first wireless FIR flight in [12], as well as piezoelectric actuated robots such as [22], [23], and [24]. In typical FIR implementation, a DC-DC switched mode converter using a high-turns ratio coupled-inductor provides the high voltage DC bias rail, and a transistor half-bridge driver alternately switches the center node V_{Sig} of the bimorph actuator between V_{Bias} and 0 V in order to achieve the desired waveform over time. The half-bridge driver is a linear

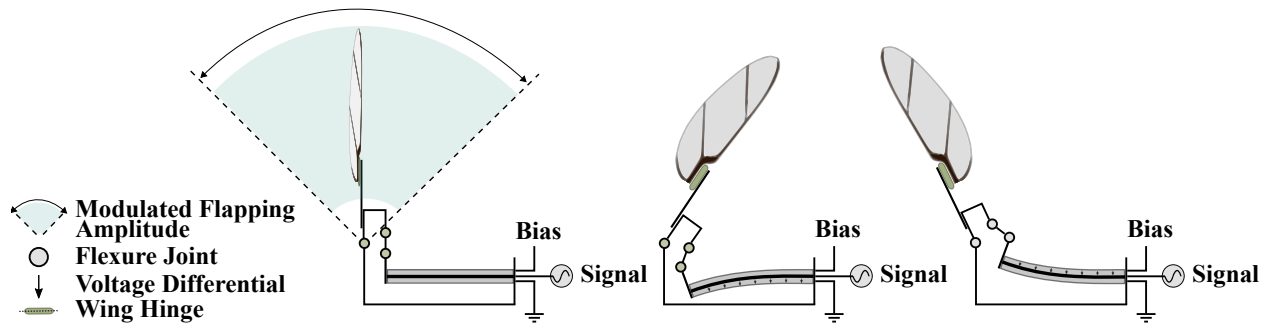


Fig. 2: Diagram showing the principle of operation of a single piezo-actuated wing in the UW Robofly. (left) A bimorph cantilever-beam piezoelectric actuator is fastened rigidly to the airframe at one end. At the other, it is connected to a transmission with a short lever arm, providing a large angular amplification of the small tip motion of the actuator. Under typical conditions, the wing amplitude is around 90° . (middle and right) As the voltage signal oscillates, the top and bottom piezo actuators are alternately charged. The resulting electric field induces a small strain in the piezoelectric material, which results in motion at the tip of the actuator. This causes the flapping motion. The wing rotates passively around a wing hinge due to aerodynamic thrust, resulting in insect-like flapping kinematics that produce lift.

driver. As such, it is inefficient for both large voltage reduction and for the piezoelectric actuator's reactive power, fundamentally because it must dump electrical charge to ground to drive negative I_{Sig} . Efficiency is further reduced when there is a large instantaneous dV_{Sig}/dt because of the piezo's capacitive reactance. Some of this energy can be recovered if additional hardware including a coil is added [21], [6], but it is uncertain whether the additional weight results in a net energy savings or not in flight.

- 2) Bi-directional power conversion and piezo drive. A bi-directional converter can incorporate the high-ratio voltage step up as well as directly drives V_{Sig} . This avoids the inefficiency of the half-bridge driver by 'recovering' power from the actuator back to the supply, as when driving negative dV_{Sig}/dt . This was demonstrated on FIRs in [13] where thin-film PV cells bathed in ≈ 3 suns of light powered a wireless (uncontrolled) sustained flight of an FIR. The downside is that a V_{Bias} rail is not supplied, and so in that particular implementation only one half of the bimorph is energized at any one time, reducing the power density of the actuator (its power produced per unit mass).

Although bi-directional power conversion is more efficient as shown in [13], that implementation sacrificed power density in the bimorph actuators, and generally requires one coil per signal in addition to a DC bias source for implementation of simultaneous drive for bimorphs [21]. Extending that topology, flight control in a two-winged robot (rather than open-loop flight) would require 4 coils. In contrast, the first topology requires only a single coil at the expense of added transistors and decreased efficiency. Given that coils are the most massive component on a PEU for an FIR, in this work we therefore have employed the first topology.

Fig. 3 gives a schematic and description of key elements of our PEU design.

DC-DC Converter and half-bridge driver

The DC-DC converter should be capable of 200 mW at 200–250 V at a current $\propto C \frac{dV_{Sig}}{dt}$ to the driver for our FIR. This work utilizes coupled-inductor boost converter topology proposed in [6], [25]. An improvement to the PEU utilized in [12] is the use of a GanFET (EPC2110, Efficient Power Conversion Corporation, El Segundo, CA) as the boost converter switching element for improved efficiency and weight, similar to [26]. Additionally, a larger capacitor, C_2 in Fig. 3 and visible in Fig. 4, was utilized to ease control of V_{Bias} .

The half-bridge driver stage consists of high-side and low-side transistor arrangements depicted in Fig. 3. As described above, the microcontroller drives these transistors in order to pull V_{Sig} towards V_{Bias} during increasing reference, or alternately to reduce V_{Sig} by sinking charge from the piezoelectric actuator to ground. PFM is used to the to drive the transistors to ensure more predictable switching in the half-bridge driver, and to avoid boost converter switching losses by using an optimal fixed pulse width.

III. METHODS

Here we describe how we created the desired waveform, measured the output of the PEU, and measured thrust from the flapping wing of an FIR. In all experiments and depicted waveforms, the V_{Sig} is set to have DC-offset equal to half the V_{Bias} command, which corresponds to a zero pitch-torque command [2], [15].

Creating arbitrary repeatable waveforms given varying loads under the constraints of an FIR-compatible PEU (Section II) required devising a means to obtain lookup tables to generate appropriate periodic pulse trains for both the driver and boost converter. We devised an iterative learning controller using an LT-Spice based simulation. This simulation implements the circuit and lumped parameter model for actuator and load shown in Fig. 3. The actuator load (equated to series RCL elements) is the Van Dyke model described in IEEE piezoelectricity standards and also detailed in [6]. The

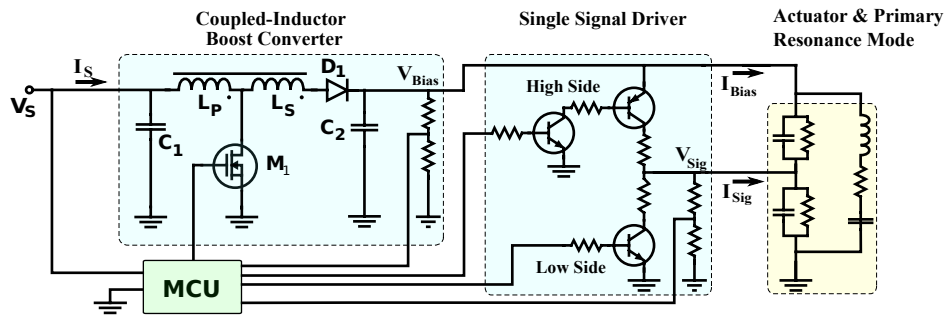


Fig. 3: PEU Circuit schematic. A microcontroller (MCU) controls the system. On the left, a coupled-inductor high-voltage DC-DC boost converter produces an approximately constant V_{Bias} . A signal driver draws from this voltage source to produce an oscillating signal V_{sig} using a half-bridge. At right is a model of the behavior of the piezoelectric bimorph actuator including resonance and air drag on the wing. For both V_{Bias} and V_{sig} , a voltage divider scales the voltage down to a range compatible with the ADC in the MCU. An iterative-learning feedback controller minimizes the difference from reference voltage. To drive a second wing, a second driver would be incorporated.

simulation results using this model were validated against the physical circuit and robot mechanism during this work. In this approach, the output of the previous cycle is stored in memory, compared to the reference signal, and linear corrections to the PFM look-up tables are made online. This repetitive learning occurs of a period of approximately 200 cycles in this work.

We then fabricated a benchtop version of the PEU (Fig. 4 and implemented the controller in C on a ST Microelectronics STM32F4 microcontroller, chosen because it provides many timers, a small (8 mg) package, and floating-point math. The voltage divider outputs from the PEU sensing circuitry were measured by the ADC of the STM32F4 microcontroller at the controller sampling frequency of 8.1 kHz. The code was debugged and tuned on a passive resistor-capacitor (RC) circuit with impedance similar to the load of the FIR's piezo actuator-wing system. The lumped-parameter coefficients modeling the FIR's wing system were found to be highly variable due to wear and varying payload, making model-based control design difficult. The RC test load, therefore, was valuable for empirical tuning even though it does not exhibit the resonance of the target load.

Voltages V_{Bias} and V_{Sig} were directly measured by oscilloscope (Rigol DS1054Z) at 10 kHz. Simultaneously, a running log of preceding 10 flapping cycles was stored in the MCU until the end of the experiment and then transmitted via UART to a custom-written NI LabVIEW software interface. Additionally, a custom circuit used isolation amplifiers (AMC1302, Texas Instruments) to measure the highside currents I_S , I_{Bias} , and I_{Sig} depicted in Fig. 3, and these measurements were logged by an NI USB digital acquisition system (DAQ) concurrently with oscilloscope measurements. Oscilloscope, MCU, and DAQ measurements were synchronized in time by measuring an additional digital timing signal produced by the MCU. Fig. 5 shows an example learned waveform driving the RC load.

To measure thrust, a single wing in a Robofly similar to [3] was driven by the PEU while mounted to a capacitive force sensor similar to that presented in [27]. This sensor measures

small displacements, read-out as changes in capacitance, of a flexible beam. This configuration provides a high-bandwidth, low-error measurement of the beam position. The beam was configured so that thrust force from the wing induced deformation along its flexible mode. The output of the capacitance meter (Microsense 8810) varies linearly with displacement and therefore applied force, and was also measured by the NI DAQ and LabVIEW software interface. To eliminate sensor drift, the electrical current and force sensors were zeroed by taking a time-averaged measurement after settling for several seconds after wing flapping ceased.

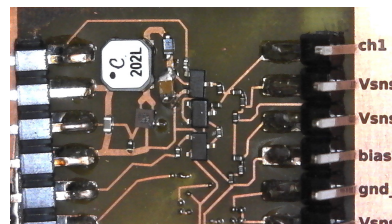


Fig. 4: Benchtop version of the PEU. Compared to the flight-weight PEU in Fig. 1, it has smaller dimensions, is on a heavier non-flex FR-4 substrate that is easier to prototype but is functionally equivalent, includes additional connections for characterization, uses a GaN FET as the the boost converter switch, uses a larger bias capacitor C_2 , and the coupled inductor's shield was not removed. The MCU is on an external PCB for ease of development. The authors previously demonstrated these components on a single flex circuit in [12].

All thrust experiments were done at 240 V bias, near the 250 V maximum voltage rating of the PEU's components. This maximizes potential thrust and control authority but reduces boost converter efficiency.

Insofar as end-to-end efficiency, because the half-bridge driver loses reverse-power (i.e. dumps to ground any negative I_{Sig}), we have zeroed the reverse power as in [1] and do not consider negative power to be 'returned'. Using measured currents as indicated in Fig. 3, with $\hat{I}_{Sig} = \max(0, I_{Sig})$, and \bar{x} as the time average, taken over 10-cycles, end-to-end efficiency is given by:

$$\eta = \frac{(V_{Sig}\hat{I}_{Sig} + V_{Bias}I_{Bias})}{(V_s I_s)} \quad (1)$$

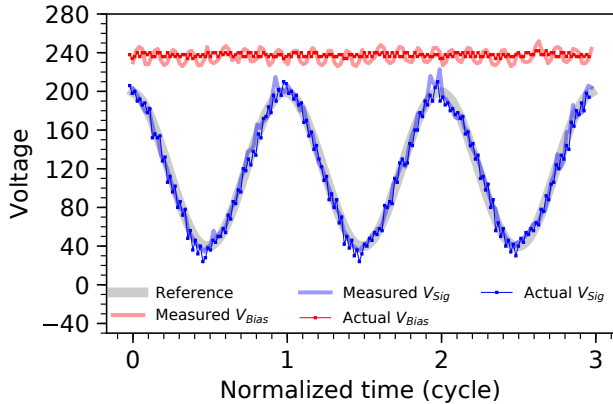


Fig. 5: Typical voltage over time normalized to the period of one wing-stroke, from the PEU driving the RC ‘dummy’ load, showing that it follows the reference signal well. Settings: frequency 160 Hz, 160 V_{pp} , 120 V_{DC} offset from gnd, and bias signal $V_{Bias} = 240$ V. Oscilloscope measurements (“Actual”) assumed to be ground truth are overlain, showing agreement with online ADC measurements (“Measured”) made by the MCU. The abscissa is time normalized to the period of one wing stroke.

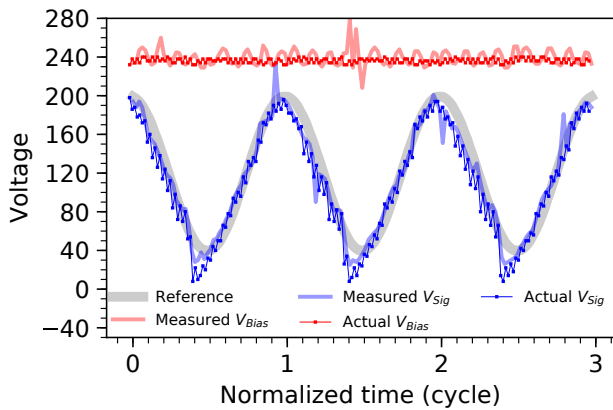


Fig. 6: Typical waveform from the PEU driving a Robofly wing to follow a sinusoidal reference signal, showing slightly diminished performance relative to the RC load. Waveform settings are the same as in Figure 5.

IV. RESULTS

The estimated weight of our PEU excluding interchangeable microcontroller but including flex PCB, larger bias storage capacitor, and dual drivers is 90 mg, fitting within the payload budget of a <500 mg flying insect robot (FIR).

Fig. 7 shows that the PEU is capable of producing signals across a range of desired amplitudes. Relatively good control of V_{Bias} , V_{Sig} can be observed as a relatively small deviation from reference and a nearly constant DC bias voltage, despite the large range of instantaneous boost converter power throughout the flapping cycle.

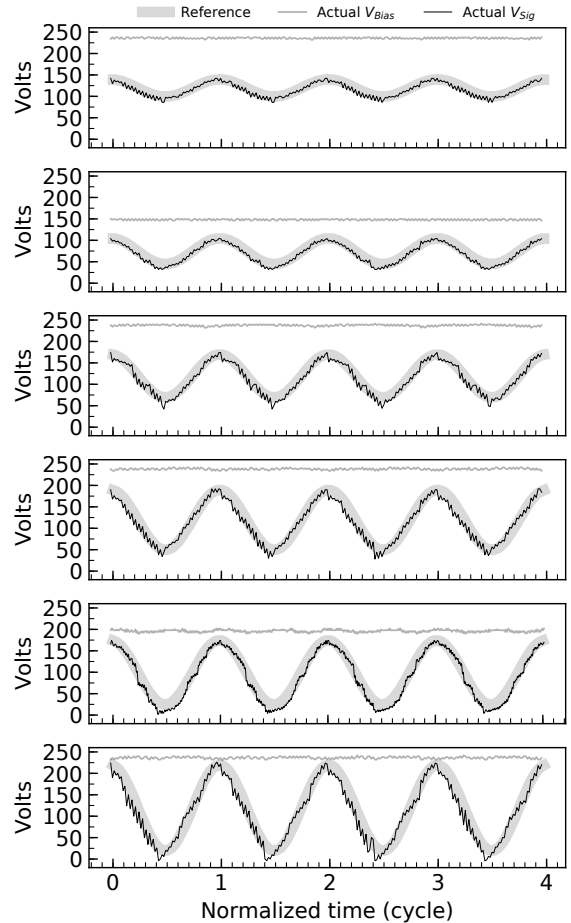


Fig. 7: The PEU can consistently produce waveforms across a range of desired amplitudes and V_{Bias} , while maintaining a nearly constant V_{Bias} . From top-to-bottom, the V_{Bias}/V_{Sig} set-points are respectively: 240/40; 150/60; 240/100; 240/140; 200/150; 240/200.

A. Waveform quality

The flight mechanics of FIRs and insects alike require smooth wing motion to maximize lift and minimize wear on the mechanism. piezoelectric actuators are extremely high-bandwidth which is advantageous for control [28]. But it also means that distortion of the V_{Sig} is transmitted directly to the actuator, and the wings. It is desirable to avoid high frequency content of the waveform because the half-bridge driver topology is inefficient with reactive power, and the piezoelectric actuators can be easily damaged by discontinuous V_{Sig} , V_{Bias} or frequency content at the actuator’s resonant frequency [14]. Kinematic analysis of the wing motion at some radius from the wing root in [13], indicates that harmonic distortion is substantially filtered by the transmission and wing mechanism. Nevertheless, it is unknown how thrust and efficiency are impacted, if at all, by harmonic distortion.

Fig. 8 shows a Fourier decomposition of the 160 V_{pp} commanded waveform shown in Fig. 6 for 10 cycles. It shows moderate frequency content far away from the fundamental frequency of the reference signal, with a total harmonic

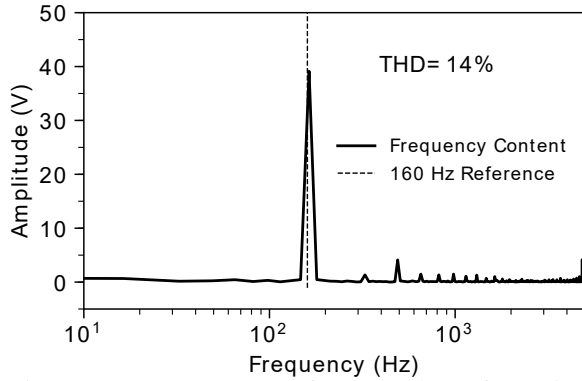


Fig. 8: Frequency content of measured V_{Sig} from Fig. 6 over 10 wing-flapping cycles.

distortion (THD) of 14%, which includes quantization effects. The waveform applied to the RC test load depicted in Fig. 5, had the benefit from more cycles of controller training, and is visibly superior with a lower THD of 8%. The contribution of measurement noise is difficult to know with certainty, given the measurement apparatus, but it is conjectured to represent a non-negligible component of the waveform’s harmonic content. Excessive low-side actuation at $t = 1.4$ cycles in Fig. 6 results in V_{Sig} error, V_{Bias} droop due to loading, and self-induced measurement noise.

Assuming the oscilloscope’s direct measurements of V_{Bias} and V_{Sig} are ground truth, the microcontroller’s measurements are noisier (Figs. 6 and 5). On FIRs, software or hardware filtering must be carefully considered due to trade-offs in computational expense and time-delays or potential loading effects on already high-impedance on-board voltage dividers for V_{Bias} , V_{Sig} .

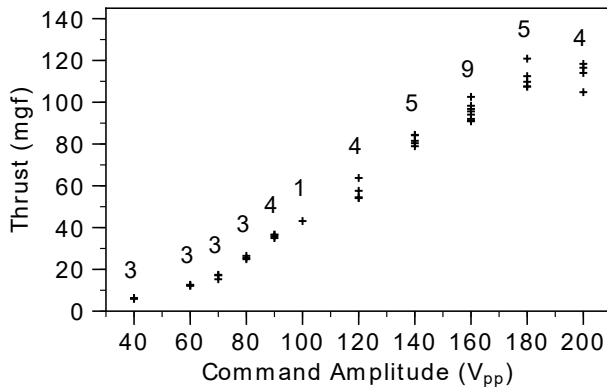


Fig. 9: Measured thrust in milligram-force is approximately linear over commanded signal amplitude. Sample size at each commanded amplitude is labeled above the data.

B. Controlled Thrust

Fig. 9 shows that wing thrust varies essentially linearly with voltage amplitude (with exceptions at very large and small amplitude). This matches previous results showed on a FIR driven with a standard benchtop piezo amplifier [29], indicating that our PEU’s output is not significantly different from a controls perspective.

As commanded amplitude decreases, the slope of the $T(V_{cmd})$ levels off as expected due to the correspondingly small stroke velocity of the wing and resultant decrease of the wing’s passive angle-of-attack and thrust generation. We conjecture that decreasing thrust per command $T(V_{cmd})$ at higher commanded amplitude > 200 V may be due to limitations of other parts of the transmission-wing system, such as wing flexing or transmission non-linearities. Although the specific slope of the $T(V_{cmd})$ and maximum thrust achieved by this half-fly is expected to vary dramatically for robots of different design and state of repair, the strong linearity of the measured thrust over commanded flapping amplitude is vital to linear controllers such as used for roll angle and altitude in [7]. This result is therefore an important step for achieving autonomous flight for FIRs.

CONCLUSIONS AND FUTURE WORK

This work reports the first PEU at a weight compatible with an FIR that is capable of modulating wing thrust. This capability is essential for flight control, because it is needed to vary lift and/or roll torque on a two-winged robot. Results were validated with thrust measurements on an FIR.

Because the system can produce arbitrary yet precisely-controlled and repeated waveform, it provides a direct path to creating the signals needed to actuate pitch and yaw torques, which are needed for attitude and position control [2], [16], [7]. Pitch and yaw torques are driven by modulating V_{Sig} ’s DC offset from $V_{Bias}/2$, and adding a 2nd harmonic content [2].

Achieving lift-to-weight ratio > 1 for our FIR carrying PEU and anticipated sensor suite [7] will require $V_{Bias} > 200$ V, $V_{Sig} > 180$ V_{pp}. The bottom waveform of Fig. 7 exceeded this, and with stroke-averaged power to the actuators of $P_{net} = 85$ mVA had an end-to-end efficiency of 20%, and boost converter efficiency of 35% when supplied with an expected supply voltage of $V_s = 7$ V as from onboard photovoltaic power sources [12]. our measured end-to-end efficiency of 20% under full load is less than the 28% reported in [13], which is expected for our half-bridge topology.

In our experience, FIRs driven by standard piezo amplifiers require trimming to eliminate bias torques [3], and demonstrate variation in thrust from robot to robot and due to mechanical wear. We anticipate that PEU calibration would entail an additional learning phase while tethered to the ground. The PEU would learn and store a number of waveforms in lookup tables (e.g. Fig. 7). In controlled flight, the PEU could then interpolate between stored tables to produce arbitrary commanded waveforms, achieving a high control bandwidth.

Our simple linear controller was able to learn how to make sinusoids with low distortion. Future improvements will reduce the weight of the output capacitor, improve the waveform, broaden the range of load impedances that can be accommodated, speed up calibration, improve signal amplitude range closer to the bias for greater control authority, use the controller look-up table adjustments to monitor load conditions, and allow the system to adapt to gradual changes from mechanical wear.

REFERENCES

- [1] Y. M. Chukewad, J. James, A. Singh, and S. Fuller, "Robofly: An insect-sized robot with simplified fabrication that is capable of flight, ground, and water surface locomotion," *arXiv preprint arXiv:2001.02320*, 2020.
- [2] K. Y. Ma, P. Chirarattananon, S. B. Fuller, and R. J. Wood, "Controlled flight of a biologically inspired, insect-scale robot," *Science*, vol. 340, no. 6132, pp. 603–607, 2013.
- [3] D. Dhingra, Y. M. Chukewad, and S. B. Fuller, "A device for rapid, automated trimming of insect-sized flying robots," *IEEE Robotics and Automation Letters*, vol. 5, no. 2, pp. 1373–1380, 2020.
- [4] Y. Zou, W. Zhang, and Z. Zhang, "Liftoff of an electromagnetically driven insect-inspired flapping-wing robot," *IEEE Transactions on Robotics*, vol. 32, no. 5, pp. 1285–1289, 2016.
- [5] P. Bhushan and C. J. Tomlin, "Milligram-scale micro aerial vehicle design for low-voltage operation," in *2018 IEEE/RSJ International Conference on Intelligent Robots and Systems (IROS)*. IEEE, 2018, pp. 1–9.
- [6] M. Karpelson, G.-Y. Wei, and R. J. Wood, "Driving high voltage piezoelectric actuators in microrobotic applications," *Sensors and actuators A: Physical*, vol. 176, pp. 78–89, 2012.
- [7] S. B. Fuller, "Four wings: An insect-sized aerial robot with steering ability and payload capacity for autonomy," *IEEE Robotics and Automation Letters*, vol. 4, no. 2, pp. 570–577, 2019.
- [8] K. Y. Ma, S. M. Felton, and R. J. Wood, "Design, fabrication, and modeling of the split actuator microrobotic bee," in *Intelligent Robots and Systems (IROS), 2012 IEEE/RSJ International Conference on*. IEEE, 2012, pp. 1133–1140.
- [9] Y. Chen, H. Wang, E. F. Helbling, N. T. Jafferis, R. Zufferey, A. Ong, K. Ma, N. Gravish, P. Chirarattananon, M. Kovac *et al.*, "A biologically inspired, flapping-wing, hybrid aerial-aquatic microrobot," *Science Robotics*, vol. 2, no. 11, 2017.
- [10] R. J. Wood, "The first takeoff of a biologically inspired at-scale robotic insect," *IEEE transactions on robotics*, vol. 24, no. 2, pp. 341–347, 2008.
- [11] S. Chaput, M. Renaud, R. Meingan, and J.-F. Pratte, "A 3.7 v to 200 v highly integrated dc-dc converter with 70.4% efficiency for portable electrostatic mems applications," in *2014 IEEE 12th International New Circuits and Systems Conference (NEWCAS)*. IEEE, 2014, pp. 381–384.
- [12] J. James, V. Iyer, Y. Chukewad, S. Gollakota, and S. B. Fuller, "Liftoff of a 190 mg laser-powered aerial vehicle: The lightest wireless robot to fly," in *2018 IEEE International Conference on Robotics and Automation (ICRA)*. IEEE, 2018, pp. 1–8.
- [13] N. T. Jafferis, E. F. Helbling, M. Karpelson, and R. J. Wood, "Untethered flight of an insect-sized flapping-wing microscale aerial vehicle," *Nature*, vol. 570, no. 7762, pp. 491–495, 2019.
- [14] B. M. Finio, N. O. Perez-Arancibia, and R. J. Wood, "System identification and linear time-invariant modeling of an insect-sized flapping-wing micro air vehicle," in *Intelligent Robots and Systems (IROS), 2011 IEEE/RSJ Int. Conf.*, September 2011, pp. 1107–1114.
- [15] Y. M. Chukewad, A. T. Singh, J. M. James, and S. B. Fuller, "A new robot fly design that is easier to fabricate and capable of flight and ground locomotion," in *2018 IEEE/RSJ International Conference on Intelligent Robots and Systems (IROS)*, Oct 2018, pp. 4875–4882.
- [16] S. B. Fuller, E. F. Helbling, P. Chirarattananon, and R. J. Wood, "Using a mems gyroscope to stabilize the attitude of a fly-sized hovering robot," 2014.
- [17] M. Karpelson, J. P. Whitney, G.-Y. Wei, and R. J. Wood, "Energetics of flapping-wing robotic insects: towards autonomous hovering flight," in *2010 IEEE/RSJ International Conference on Intelligent Robots and Systems*. IEEE, 2010, pp. 1630–1637.
- [18] N. T. Jafferis, M. A. Graule, and R. J. Wood, "Non-linear resonance modeling and system design improvements for underactuated flapping-wing vehicles," in *2016 IEEE International Conference on Robotics and Automation (ICRA)*. IEEE, 2016, pp. 3234–3241.
- [19] M. Lok, X. Zhang, E. F. Helbling, R. Wood, D. Brooks, and G.-Y. Wei, "A power electronics unit to drive piezoelectric actuators for flying microrobots," in *2015 IEEE Custom Integrated Circuits Conference (CICC)*. IEEE, 2015, pp. 1–4.
- [20] M. Lok, E. F. Helbling, X. Zhang, R. Wood, D. Brooks, and G.-Y. Wei, "A low mass power electronics unit to drive piezoelectric actuators for flying microrobots," *IEEE Transactions on Power Electronics*, vol. 33, no. 4, pp. 3180–3191, 2017.
- [21] M. Karpelson, G.-Y. Wei, and R. J. Wood, "Milligram-scale high-voltage power electronics for piezoelectric microrobots," in *2009 IEEE international conference on robotics and automation*. IEEE, 2009, pp. 2217–2224.
- [22] K. Jayaram, J. Shum, S. Castellanos, E. F. Helbling, and R. J. Wood, "Scaling down an insect-size microrobot, hamr-vi into hamr-jr," *arXiv preprint arXiv:2003.03337*, 2020.
- [23] M. Karpelson, B. H. Waters, B. Goldberg, B. Mahoney, O. Ozcan, A. Baisch, P.-M. Meyitang, J. R. Smith, and R. J. Wood, "A wirelessly powered, biologically inspired ambulatory microrobot," in *Robotics and Automation (ICRA), 2014 IEEE International Conference on*. IEEE, 2014, pp. 2384–2391.
- [24] S. A. Rios, A. J. Fleming, and Y. K. Yong, "Monolithic piezoelectric insect with resonance walking," *IEEE/ASME Transactions on Mechatronics*, vol. 23, no. 2, pp. 524–530, 2018.
- [25] *High Gain Step-up Converter with Coupled Inductor for Piezoelectric Element Drive*, Fairchild Semiconductor Corporation, 2014, rev. 1.0.
- [26] V. Iyer, A. Najafi, J. James, S. Fuller, and S. Gollakota, "Wireless steerable vision for live insects and insect-scale robots," *Science Robotics*, vol. 5, no. 44, 2020.
- [27] B. M. Finio, K. C. Galloway, and R. J. Wood, "An ultra-high precision, high bandwidth torque sensor for microrobotics applications," in *2011 IEEE/RSJ International Conference on Intelligent Robots and Systems*. IEEE, 2011, pp. 31–38.
- [28] R. J. Wood, E. Steltz, and R. Fearing, "Optimal energy density piezoelectric bending actuators," *Sensors and Actuators A: Physical*, vol. 119, no. 2, pp. 476–488, 2005.
- [29] N. O. Pérez-Arancibia, K. Y. Ma, K. C. Galloway, J. D. Greenberg, and R. J. Wood, "First controlled vertical flight of a biologically inspired microrobot," *Bioinspiration and Biomimetics*, vol. 6, no. 3, p. 036009, September 2011.